

Fractal structure of a dissipative particle-fluid system in a time-dependent chaotic flow

M. Liu,^{1,2} R. L. Peskin,^{1,*} and F. J. Muzzio^{1,2}

¹Center for Computer Aids for Industrial Productivity, Rutgers University, Piscataway, New Jersey 08855

²Department of Chemical and Biochemical Engineering, Rutgers University, Piscataway, New Jersey 08855

(Received 31 May 1994)

Motion of rigid particles under the effects of pressure force, added mass effect, and Stokes drag is investigated in the incompressible, time-dependent flow in a two-dimensional rectangular cavity. It is shown that rigid particles in a viscous flow constitute a dissipative system with a negative volume contraction exponent and become trapped by strange attractors. Two methods are used to compute Lyapunov exponents of particle motion, and several methods are used for fractal dimensions of the attractors. Results obtained from these methods are in good agreement with each other.

PACS number(s): 47.55.Kf, 47.52.+j, 47.53.+n, 47.15.Rq

Passive tracers in a fluid flow comprise a class of dynamical systems widely encountered in nature, science, and engineering. Examples include the transport of pollutants in the atmosphere and the ocean, experimental flow visualization techniques, and multiphase flows used in chemical and petrochemical processes. Several recent studies have focused on the dynamics of particle motion in both laminar and turbulent flows as predicted by different approximated versions of the particle equations of motion, and a variety of particle behaviors, both chaotic and regular, have been identified [1–4]. However, in most of these studies, the fluid flow field was assumed to be steady; by and large, the effects of time-dependent flow fields on particle motion have not been discussed. Moreover, many of the flows investigated in these studies were based on highly simplified models, and the applicability of previously obtained results to real systems is uncertain.

This paper communicates several results concerning the motion of small rigid particles in realistic fluid flows. It is shown here the such motions can be dissipative and generate strange attractors for a variety of flow and particle conditions. The physically realizable flow in a two-dimensional rectangular cavity with an aspect ratio of $H/L=0.6$, where H is the height of the vertical walls and L is the width of the horizontal walls, is chosen as a case study. The flow is incompressible and time-dependent and is the combination of two piecewise steady flows generated by alternatively moving each of the horizontal walls for a fixed amount of time while keeping the vertical walls stationary (a detailed description of this flow has been provided elsewhere; see Refs. [5,6]). The main flow parameter T is defined as the combined displacement of both horizontal walls during one period divided by the length of the cavity. Our study is restricted to cases with a Reynolds number $Re=\rho_F UL/\mu < 1.0$, where ρ_F is the fluid density, μ is the fluid viscosity, and U is the wall velocity. This range of Re yields a creeping flow with minimal inertial forces. Since no analytical

solution is available, the flow field is obtained numerically using a finite difference scheme to solve the full Navier-Stokes equations. As is shown elsewhere [6], simulated mixing results agree well with experiments [5].

In this study, small rigid spherical particles are treated as passive tracers, i.e., the effect of particles on the flow field is not considered. Particle concentration is small, and particle-particle interactions are neglected. We adopt the particle equation of motion derived by Maxey and Riley for particles moving under the effects of pressure force, added mass effect, and Stokes drag [7]. For a steady flow, this equation can be rearranged and nondimensionalized as

$$\frac{d\mathbf{v}}{dt} = (1/S_{\text{drag}})[\mathbf{u} - \mathbf{v}] + M[\mathbf{u} + \mathbf{v}/2] \cdot \nabla \mathbf{u}, \quad (1)$$

where \mathbf{u} is the fluid velocity and \mathbf{v} is the particle velocity. The parameter $S_{\text{drag}} = (1+2\gamma)a^2 Re / (9L^2)$ indicates the relative importance of Stokes drag (for a given flow, a larger value of S_{drag} indicates a larger or a heavier particle), and $M = 2/(2\gamma+1)$, where $\gamma = \rho_P/\rho_F$, a is the particle radius, and ρ_P is the particle density. Equation (1) is strongly nonlinear and for most flows must be integrated numerically to obtain the particle velocity. Particle trajectories can then be found by integrating the equation $d\mathbf{x}/dt = \mathbf{v}$.

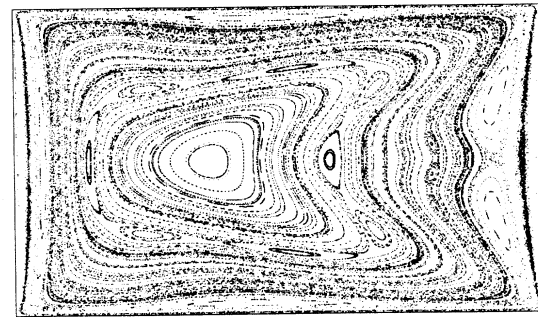
In a recent experimental study, Sommerer and Ott [2] showed that solid particles floating in the free surface of a fluid can form strange attractors. They argued that such attractors occurred because particles were restricted to the surface of the fluid, and the divergence of such two-dimensional (2D) motions can differ from zero, even if the fluid is incompressible. The main point of this paper is to show that strange attractors for motion of solid particles can occur under much more general conditions. Fluid particles in the truly 2D cavity flow have two degrees of freedom, i.e., description of their motion requires a 2D phase space, which is also the physical space. If the flow is incompressible, the volume change in phase space is $\nabla \cdot \mathbf{u} = 0$, the system is conservative, and the stream function plays the role of the Hamiltonian. On the other hand, as is evident in Eq. (1), the motion of rigid particles in a 2D flow has four degrees of freedom, i.e., it is embed-

*Author to whom all correspondence should be sent.

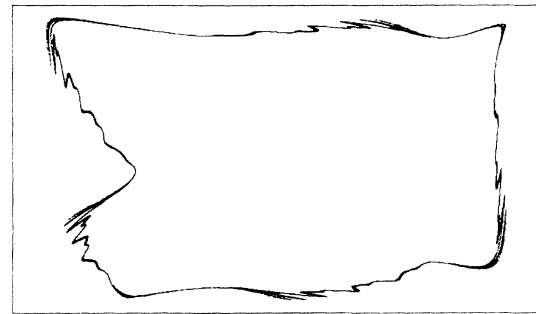
ded in a four-dimensional (4D) phase space. The particle system is no longer conservative; the rate of change of phase space volume \mathcal{V} is $(1/\nu)D\mathcal{V}/Dt = -2/S_{\text{drag}}$. For the cases examined in this paper, $S_{\text{drag}} < 1.0$, and the system is strongly dissipative. Moreover, $\nabla \cdot \mathbf{v} \neq 0$ even for descriptions restricted to the 2D physical space, indicating that strange attractors are possible for rigid particles both in the 4D phase space and in the 2D physical space. In the more restricted context of the cavity flow, while light particles ($\gamma \ll 1$) converge to a point attractor for a wide range of S_{drag} , heavy particles ($\gamma \gg 1.0$) are repelled to the boundary walls. However, for $\gamma \sim 1$, rigid particles are often attracted either to quasiperiodic orbits or to chaotic attractors.

Since previous studies have shown that fluid particles undergo chaotic motion in the cavity flow for a wide range of T [5,6], it is not surprising to observe chaotic motion of rigid particles in this flow. However, chaotic fluid motion and chaotic rigid particle motion show significant differences. Figure 1(a) shows the Poincaré section for the fluid particles in a periodic cavity flow at $T=2.0$. The points in the figure are particle positions at the end of each period. The flow is mostly regular, except in narrow layers, the largest of which is readily observed close to the cavity boundaries. Figure 1(b) shows a Poincaré section for rigid particles ($S_{\text{drag}}=0.2$, $\gamma=1.3$) under the same flow conditions. The figure was computed by placing a single particle at $(x_0, y_0)=(0.7, 0.3)$ and following it for 60 000 periods. The particle undergoes chaotic motion within a fractal attractor. The structure of this attractor is significantly different than the structure of Kolmogorov-Arnold-Moser (KAM) surfaces and chaotic regions in the underlying flow. Comparison of Figs. 1(a) and 1(b) readily reveals that the rigid particle repeatedly crosses KAM surfaces of the underlying flow.

A wide variety of attractor structures are observed for different flow conditions. Figure 1(c) shows a rigid particle Poincaré section corresponding to $T=4.2$, $S_{\text{drag}}=0.2$, $\gamma=0.5$. Once again, the rigid particle is confined to an attractor. Empty regions of different sizes coexist with regions populated by points, suggesting a fractal attractor structure. Additional cases (now shown here) demonstrate that the structure of the attractors depends strongly on flow conditions. It should be pointed out that particle attractors are not the product of periodicity; they also exist for aperiodic flows. Poincaré sections cannot be used to investigate such cases, but attractors can be generated using an alternative strategy where 40 000 rigid particles, initially distributed uniformly in the entire flow domain, are followed in time. The structure occupied by the particles at a given time has been termed a "snapshot attractor" [2]. Numerical results show that a snapshot attractor approaches the Poincaré attractor after a brief transient whose duration depends on all three parameters S_{drag} , γ , and T . In general, the more tenuous the attractor, the shorter the transient. Figure 1(d) shows the snapshot attractor generated by an aperiodic "symmetry breaking" sequence of wall motions *abbabaabbaababba* . . . [8], where "a" indicates motion of the top wall and "b" indicates motion of the bottom wall. Each wall motion lasts a time $T/2=2.1$, and parti-



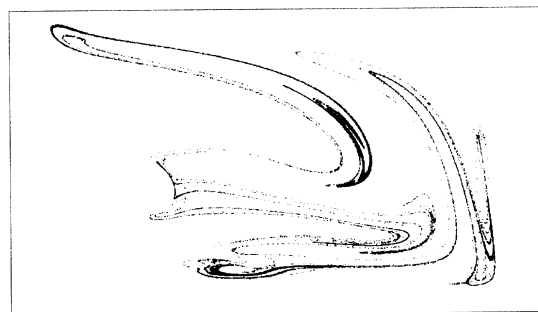
(a)



(b)



(c)



(d)

FIG. 1. (a) Poincaré section for fluid particles, $T=2.0$; (b) Poincaré section for rigid particles, $T=2.0$, $S_{\text{drag}}=0.2$, and $\gamma=1.3$; (c) Poincaré section for rigid particles, $T=4.2$, $S_{\text{drag}}=0.2$, and $\gamma=0.5$; (d) "snapshot attractor" for rigid particles in a symmetry-breaking flow, $T=4.2$, $S_{\text{drag}}=0.2$, $\gamma=0.5$, for a total time of $15T$.

cle properties correspond to $S_{\text{drag}}=0.2$, $\gamma=0.5$. As is shown in Fig. 1(d), the rigid particles converge at an attractor whose topology resembles that observed in Fig. 1(c) for the corresponding periodic case.

To qualify as strange attractors, the structures in Fig. 1 should exhibit (i) a positive largest Lyapunov exponent along particle trajectories and (ii) a fractal dimension. Both of these conditions are satisfied for the systems studied here. We begin with the analysis of the Lyapunov exponent $\lambda_i = \lim_{t \rightarrow \infty} \{(1/t) \ln[l(t)/l(0)]\}$, where $l(t)$ is the distance between two neighboring particles at time t . Two Lyapunov exponents can be found for trajectories in the 2D physical space. If the system is chaotic, the largest exponent λ_1 must be positive. A simple relation exists between the Lyapunov exponents λ_1 , λ_2 and the volume contraction exponent σ , i.e., $\sigma = \lim_{t \rightarrow \infty} \{(1/t) \ln[\Delta A(t)/\Delta A(0)]\} = \lambda_1 + \lambda_2$, where $\Delta A(t)$ is a differential of area in physical space. For a dissipative system, $\lambda_1 > 0$, $\lambda_2 < 0$, $|\lambda_2| > |\lambda_1|$, and $\sigma < 0$.

Two different methods have been used to compute Lyapunov exponents. In the first method, $l(t)$ and $\Delta A(t)$ are computed directly from the equations

$$\frac{dl(t)}{dt} = l(t) \cdot (\nabla \mathbf{v}), \quad \frac{d\Delta A(t)}{dt} = \Delta A(t) (\nabla \cdot \mathbf{v}); \quad (2)$$

the velocity derivatives needed for $\nabla \mathbf{v}$ and $\nabla \cdot \mathbf{v}$ are obtained by differentiating Eq. (1) along particle trajectories. In the second method, five particle trajectories are followed in the 4D phase space; one of the trajectories is chosen as a reference, and $l(t)$ is found from the distances of the remaining four trajectories to the reference trajectory. Lyapunov exponents are then obtained using a Gram-Schmidt renormalization procedure [9]. The two methods give almost identical results. Computations for $(T, S_{\text{drag}}, \gamma) = (2.0, 0.2, 1.3)$ yield $\lambda_1 = 0.023 \pm 0.002$, $\lambda_2 = -0.086 \pm 0.001$, and $\sigma = -0.063 \pm 0.003$; similarly, for $(T, S_{\text{drag}}, \gamma) = (4.2, 0.2, 0.5)$, one gets $\lambda_1 = 0.115 \pm 0.002$, $\lambda_2 = -0.209 \pm 0.002$, and $\sigma = -0.094 \pm 0.004$. Since σ is the long-time average of $\nabla \cdot \mathbf{v}$, these results show that $\nabla \cdot \mathbf{v} < 0$, demonstrating that strange attractors are indeed possible for the rigid particle system.

To qualify as strange attractors, the rigid particle structures in Fig. 1 must also be characterized by a fractal dimension. Qualitatively, the structures in Fig. 1 “look fractal,” i.e. they display a wide length scale distribution, and enlarged portions of each structure resemble the whole structure [4]. To examine this point quantitatively, six different dimensions were calculated using four numerical schemes. The first scheme, “box-counting,” was used to compute the capacity dimension d_c , the information dimension d_I , and the correlation dimension d_{corr} [10]. The attractor must have at least 300 000 points for this scheme to give reasonably accurate results. The second scheme computes the distances between all possible pairs of points in the attractor and obtains the correlation dimension d_{cor} from the slope of the probability density function of distances [10]. Although it is computationally costly to calculate the distance of every pair

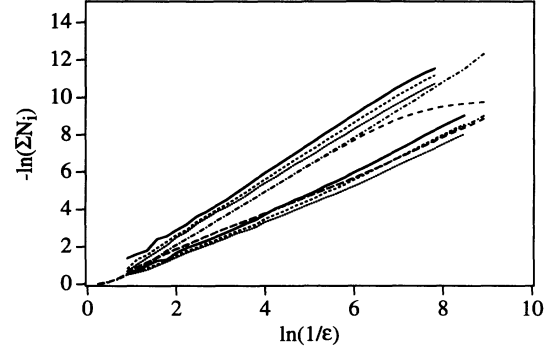


FIG. 2. Fractal dimension of strange attractors (solid line, d_c ; short dashes, d_I ; small dots, d_{corr} ; long dashes, d_{cor} ; and dash-dots, d_L). The upper group of curves corresponds to $(T, S_{\text{drag}}, \gamma) = (4.2, 0.2, 0.5)$. The slopes of the curves yield the dimensions $d_c = 1.580 \pm 0.005$, $d_I = 1.530 \pm 0.004$, $d_{\text{corr}} = 1.460 \pm 0.002$, $d_{\text{cor}} = 1.430 \pm 0.003$, $d_r = 1.440 \pm 0.002$, and $d_L = 1.55 \pm 0.02$. The lower group of curves corresponds to $(T, S_{\text{drag}}, \gamma) = (2.0, 0.2, 1.3)$ and yields the dimensions $d_c = 1.160 \pm 0.003$, $d_I = 1.130 \pm 0.002$, $d_{\text{corr}} = 1.060 \pm 0.004$, $d_{\text{cor}} = 1.060 \pm 0.005$, $d_r = 1.040 \pm 0.005$, and $d_L = 1.26 \pm 0.02$.

of points, this scheme gives accurate results with just 10 000 points in the attractor. In the third scheme, a small number of locations, N_r , is chosen randomly, a circular domain of radius ϵ is centered at each location, and $N_i(\epsilon)$, the number of points in each domain, is computed. The fractal dimension d_r is then obtained from the slope of a plot of the number of points inside a domain vs the domain radius. The last scheme computes the fractal dimension d_L from the Kaplan-Yorke conjecture, which for a 2D system is $d_L = 1 + \lambda_1/|\lambda_2|$, where λ_1 and λ_2 are the positive and negative Lyapunov exponents.

Results from these schemes are shown in Fig. 2 for the same two cases as in Figs. 1(b) and 1(c). The lower group of curves corresponds to $(T, S_{\text{drag}}, \gamma) = (2.0, 0.2, 1.3)$, and the upper group corresponds to $(T, S_{\text{drag}}, \gamma) = (4.2, 0.2, 0.5)$; the slope of the curves are the fractal dimensions. All of the curves display linear ranges, indicating well defined fractal behavior. Moreover, since each group of curves has about the same slope, the figures demonstrate good agreement between the various dimensions. The attractor corresponding to $(T, S_{\text{drag}}, \gamma) = (2.0, 0.2, 1.3)$ has a dimension of about 1.1, and the attractor for $(T, S_{\text{drag}}, \gamma) = (4.2, 0.2, 0.5)$ has a dimension of about 1.5. The three dimensions obtained from box counting are in consistent order $d_c \geq d_I \geq d_{\text{corr}}$. It is also apparent that $d_{\text{corr}} \approx d_{\text{cor}} \approx d_r$. This is expected, since these dimensions have similar physical meanings. The relation of d_L to the rest of each group is not clear. While for $(T, S_{\text{drag}}, \gamma) = (4.2, 0.2, 0.5)$, $d_L \approx d_I$ as predicted by Ledrappier and Young [11], for $(T, S_{\text{drag}}, \gamma) = (2.0, 0.2, 1.3)$ d_L is about 10% larger than any of the other dimensions. However, the remaining five dimensions are in close agreement with one another.

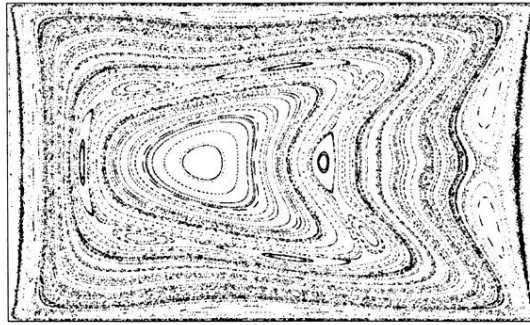
In summary, it is shown that rigid particles in a viscous flow constitute a dissipative system and can

display strange attractors, and that while two-dimensional time-periodic flows generate chaotic motions of rigid particles, the structure of such motions exhibits strong differences from the structure of the underlying flow. These differences are important for many practical applications involving rigid particles; a noteworthy example is risk assessment in scenarios involving airborne particulate pollutants. As should be clear from the preceding discussion, it is important to represent the motion of rigid particles accurately, because qualitative predictions

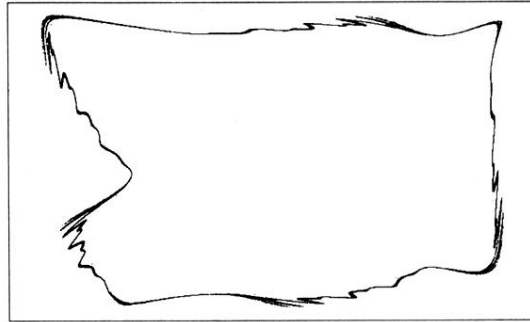
based on the structure of the underlying flow pattern can contain large errors.

This research was sponsored by NSF Grant No. ECS-9110424 for R.L.P. and by support for F.J.M. from the Exxon Education Foundation, the Merck Foundation, and Rutgers' CAIP Center. Dr. Sandra Walther at CAIP developed the scientific data management and visualization tools used in the research under NSF Grant No. IRI-9116558.

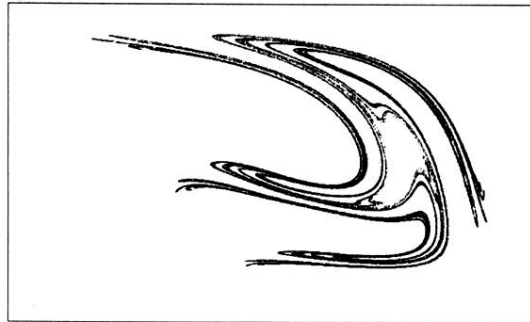
-
- [1] A. Crisanti and M. Falcioni, *Phys. Fluids A* **4**, 1805 (1992); O. A. Druzhinin, L. A. Ostrovsky, and Y. A. Stepanyants, *Chaos* **3**, 359 (1993).
- [2] J. C. Sommerer and E. Ott, *Science* **259** (2), 335 (1993).
- [3] K.-K. Tio, A. Linan, J. C. Lasheras, and A. M. Ganan-Calvo, *J. Fluid Mech.* **254**, 671 (1993); L. P. Wang, M. R. Maxey, T. D. Burton, and D. E. Stock, *Phys. Fluids A* **4**, 1789 (1992); L. Yu, E. Ott, and Q. Chen, *Physica D* **53**, 102 (1991).
- [4] M. Liu and R. L. Peskin, in *Gas-Solid Flows*, edited by D. E. Stock *et al.* (ASME, New York, 1993), Vol. 166, p. 95.
- [5] C. W. Leong and J. M. Ottino, *J. Fluid Mech.* **209**, 463 (1989).
- [6] M. Liu, R. L. Peskin, F. J. Muzzio, and C. W. Leong, *AIChE J.* **40**, 1273 (1984).
- [7] M. R. Maxey and J. J. Riley, *Phys. Fluids* **26**, 883 (1983).
- [8] J. G. Franjione, C. W. Leong, and J. M. Ottino, *Phys. Fluids A* **1**, 1172 (1989).
- [9] A. Wolf, J. B. Swift, H. L. Swinney, and J. A. Vastano, *Physica D* **16**, 285 (1985).
- [10] T. S. Parker and L. O. Chua, *Practical Numerical Algorithms for Chaotic Systems* (Springer-Verlag, New York, 1989).
- [11] F. Ledrappier and L.-S. Young, *Commun. Math. Phys.* **117**, 529 (1988).



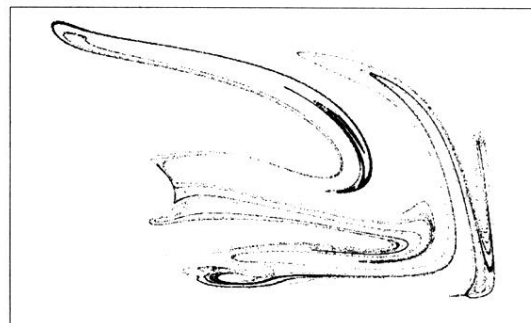
(a)



(b)



(c)



(d)

FIG. 1. (a) Poincaré section for fluid particles, $T=2.0$; (b) Poincaré section for rigid particles, $T=2.0$, $S_{\text{drag}}=0.2$, and $\gamma=1.3$; (c) Poincaré section for rigid particles, $T=4.2$, $S_{\text{drag}}=0.2$, and $\gamma=0.5$; (d) “snapshot attractor” for rigid particles in a symmetry-breaking flow, $T=4.2$, $S_{\text{drag}}=0.2$, $\gamma=0.5$, for a total time of $15T$.